Journal of Alloys and Compounds 509 (2011) 1029–1034

Contents lists available at ScienceDirect

Journal of Alloys and Compounds

journal homepage: www.elsevier.com/locate/jallcom

# Carbon nanotubes-supported PtAu-alloy nanoparticles for electro-oxidation of formic acid with remarkable activity

Yan-Cui Bai [a], Wei-De Zhang [a,*], Cai-Hong Chen [a], Jia-Qi Zhang [b]

[a] Nano Science Research Center, School of Chemistry and Chemical Engineering, South China University of Technology, 381 Wushan Road, Guangzhou 510640, People's Republic of China

[b] College of Environmental Science and Safety Engineering, Tianjin University of Technology, Tianjin 300071, People's Republic of China

ARTICLE INFO

*Article history:*
Received 25 July 2010
Received in revised form 1 September 2010
Accepted 3 September 2010
Available online 23 October 2010

*Keywords:*
Multi-walled carbon nanotubes
PtAu-alloy nanoparticles
Electro-oxidation
Formic acid

ABSTRACT

PtAu-alloy nanoparticles supported on multi-walled carbon nanotubes (MWCNTs) were successfully prepared by simultaneous reduction of $H_2PtCl_6{\cdot}6H_2O$ and $HAuCl_4{\cdot}3H_2O$ with sodium borohydride as a reducing reagent and sodium citrate as a stabilizing reagent. The morphology and composition of the composite catalyst were characterized by transmission electron microscopy, X-ray photoelectron spectroscopy and X-ray diffraction. The results show that the PtAu alloy nanoparticles with an average diameter of about 3.5 nm and narrow size distribution are supported on MWCNTs. Electrocatalytic oxidation of formic acid at the PtAu/MWCNTs nanocomposite electrode was investigated in a solution containing 0.50 M $H_2SO_4$ as a supporting electrolyte and 0.50 M formic acid by cyclic voltammogram and chronoamperometry. The results demonstrate that the PtAu/MWCNTs catalyst exhibits higher activity and stability for electro-oxidation of formic acid than the commercial Pt/C catalyst, reflecting by its lower onset potential (−0.05 V), oxidation mainly occurring in low potential range of $-0.05 \pm 0.65$ V and higher peak current density of 3.12 mA $cm^{-2}$. The result of CO stripping voltammetry discloses that gold in the PtAu/MWCNTs nanocomposite enhances the catalytic activity and stability.



## 1. Introduction

Recently, formic acid (HCOOH) has been attracting great attention as a promising alternative fuel for liquid fuel cells due to its diverse advantages, such as higher electrochemical activity, less poisoning to electrocatalysts and lower crossover through Nafion membrane than methanol [1–3]. Among the catalysts employed in the anode, platinum and palladium or their alloys have been well known as essential and the most effective catalysts. Studies on catalysts, such as Pt, PtRu [4], PtPd [5], PtPb [6], PtSn [7], PtBi [8], Pd [9] have been reported. These examples disclose that generally bimetallic catalysts often show an improved electrocatalytic performance on the basis of a bifunctional mechanism, an electronic effect, or an ensemble effect [10–12]. Gold (Au) has long been known to be catalytically far less active than other transition metals. However, it was found that when dispersed as ultrafine particles and supported on some metal oxides, Au exhibits an extraordinarily high activity for some redox reactions [13]. Nanoparticles of Au or Au-based alloys have been used as electrocatalysts. Sung and co-workers investigated PtAu alloy as an anodic catalyst in the direct liquid (methanol and HCOOH) fuel cell [14], presenting higher activity than that of commercial PtRu. Afterward, Tak and co-workers [15] studied the influence of Au contents on the performance of direct formic acid fuel cell with AuPt anode catalyst, showing that the maximum power density of $Au_{0.6}Pt_{0.4}$-based membrane-electrode-assembly was 30% higher than that of commercial $Pt_{0.5}Ru_{0.5}$-based membrane-electrode-assembly at 60 °C in 9.0 M HCOOH. Moreover, utilization efficiency of Pt can be greatly enhanced by coating on gold nanoparticles [16]. In view of reducing noble metal loading and the system cost, increasing attention has been paid to the search for employing metallic nanoparticles on different types of carbon supporting materials such as active carbon, single-walled carbon nanotubes (SWCNTs), multi-walled carbon nanotubes (MWCNTs), and graphite carbon nanofibers (GCNFs). Especially, many researchers have shown a considerable interest in using carbon nanotubes as the supporting materials, because of their nanometer size, high-accessible surface area, good electric conductivity, and outstanding mechanical properties [17]. Some metals and their compounds, such as Pt, Pd, Ru, Ni, Cu, have been successfully deposited on carbon nanotubes by means of precipitation, impregnation and electrodeposition, etc. [18–22].

Herein, we take full advantages of both MWCNTs and PtAu alloy. PtAu/MWCNTs nanocomposite was prepared successfully by simultaneous reduction of $H_2PtCl_6{\cdot}6H_2O$ and $HAuCl_4{\cdot}3H_2O$ with sodium borohydride ($NaBH_4$) as a reducing reagent, and sodium citrate as a stabilizing reagent, which is a facile and green approach.

* Corresponding author. Tel.: +86 20 8711 4099; fax: +86 20 8711 2053.
*E-mail address:* zhangwd@scut.edu.cn (W.-D. Zhang).

0925-8388/$ – see front matter © 2010 Elsevier B.V. All rights reserved.
doi:10.1016/j.jallcom.2010.09.165

The electrocatalytic performance of the prepared PtAu/MWCNTs was evaluated by cyclic voltammetry (CV) and amperometry in a mix solution of 0.50 M HCOOH and 0.50 M $H_2SO_4$. The results show that the PtAu/MWCNTs catalyst presents excellent electrocatalytic activity for the oxidation of formic acid. Meanwhile, the role of gold in the PtAu/MWCNTs nanocomposites was also studied by CO stripping voltammetry. The experimental results of this study provide a promising application of formic acid as a fuel for fuel cell.

## 2. Experimental

### 2.1. Chemicals and materials

MWCNTs were customer-made by catalytic chemical vapor deposition [23]. $H_2PtCl_6{\cdot}6H_2O$, $HAuCl_4{\cdot}3H_2O$ were purchased from Sigma–Aldrich and Nafion (5.0 wt%) from Alfa Aesar. Commercial carbon-supported Pt nanoparticles (Pt/C, 2.3 nm) with a mass ratio of 46.3 (Pt) to 53.7 (C) were purchased from Tanaka Kikinzoku Kogyo Co. Ltd. Japan. Pure nitrogen ($N_2$, 99.99%) and carbon monoxide (CO, 99.9%) were used in the experiments. All other reagents were of analytical grade and used without further purification. All solutions were prepared with high-quality deionized (DI) water (18.4 MΩ $cm^{-1}$).

### 2.2. Apparatus

The morphological characterization of Pt@Au/MWCNTs was investigated by transmission electron microscopy (TEM, Philips CM 300 FEG), X-ray photoelectron spectroscopy (XPS, Kratos, Axis Ultra DLD) and a Shimadzu XD-3A X-ray diffractometer (XRD) with Cu Kα radiation (λ = 1.5406 nm). Electrochemical experiments were carried out with a CHI660C electrochemical workstation (Shanghai Chenhua, China).

### 2.3. Synthesis of PtAu/MWCNTs nanocomposite

Previous to the synthesis of PtAu/MWCNTs, MWCNTs were functionalized according to a previous report [24]. Briefly, an appropriate amount of MWCNTs were immersed in a 3:1 mixture of concentrated nitric acid ($HNO_3$) and sulphuric acid ($H_2SO_4$), and sonicated for 4.0 h. Then, the mixture was washed with a large quantity of DI water until the washings showed no acidity and then dried in the oven. Some oxygen-containing functional groups, such as quinonyl, carboxyl, or hydroxyl groups, occurred on the oxidatively pretreated MWCNTs, which further advances the nanoparticles' deposition onto the MWCNTs.

The PtAu/MWCNTs catalyst with 15% overall metallic mass content was prepared by simultaneous reduction of $H_2PtCl_6{\cdot}6H_2O$ and $HAuCl_4{\cdot}3H_2O$ precursors in one step by a modified approach based on a previous report [25]. In brief, 14.68 mg functionalized MWCNTs were firstly dispersed into 10 mL ethanol under ultrasonication for half an hour. 20 mL ethanol solution containing $5.0 \times 10^{-4}$ M $H_2PtCl_6{\cdot}6H_2O$, $2.5 \times 10^{-4}$ M $HAuCl_4{\cdot}3H_2O$ and $7.5 \times 10^{-4}$ M sodium citrate was added to the MWCNTs suspension and stirred sufficiently. Subsequently, 1.2 mL of ice-cold, freshly prepared 0.10 M $NaBH_4$ solution (prepared in NaOH solution with pH 12.0) was added to the above mixture rapidly. After that, the mixture was stirred for an additional 20 h at room temperature. Finally, the mixture was centrifuged, washed with DI water, and then dried in an oven at 70 °C. During the process, $PtCl_6^{2-}$ and $AuCl_4^-$ were reduced to metallic Pt and gold, with $BH_4^-$ being reducing reagent, which is the source of electrons while sodium citrate acts as a stabilizing reagent for controlling the particle growth [26]. For comparison, Pt/MWCNTs and Au/MWCNTs catalysts were also prepared by the same way. The detailed process for preparation of electrode based on the prepared PtAu/MWCNTs was reported in our previous work [21].

### 2.4. Electrochemical measurement

Electrochemical experiments were carried out on a conventional three-electrode system with a PtAu/MWCNTs modified GC electrode (3.0 mm in diameter) as working electrode, a platinum wire as counter electrode and an Ag/AgCl (3.0 M KCl) electrode as reference electrode. The CV experiments were performed in 0.50 M $H_2SO_4$ solution containing 0.50 M HCOOH at a scan rate of 50 mV $s^{-1}$. In all of the experiments, stable voltammogram curves were recorded after scanning for about 40 cycles in the potential region from −0.2 V to +1.0 V. All potentials reported in this article were referred to the Ag/AgCl. All measurements were performed at ambient temperature. The solutions were deaerated by purging with high-purity nitrogen. During the measurement, nitrogen was passed through the solution.

The CO stripping voltammogram was performed in 0.50 M $H_2SO_4$ solution with a three-electrode cell. Firstly, $N_2$ gas was purged to 0.50 M $H_2SO_4$ solution for 30 min to remove the dissolved $O_2$. Then, CO gas was purged to the 0.50 M $H_2SO_4$ solution for 15 min to get a CO monolayer adsorption saturated electrode by maintaining the electrode potential at +0.07 V. Subsequently, the dissolved CO in the solution was removed by bubbling $N_2$ into the solution for 30 min again. Linear sweep voltammetry (LSV) was carried out in 0.50 M $H_2SO_4$ solution from −0.20 V to +1.0 V *vs* Ag/AgCl at a scan rate of 20 mV $s^{-1}$.

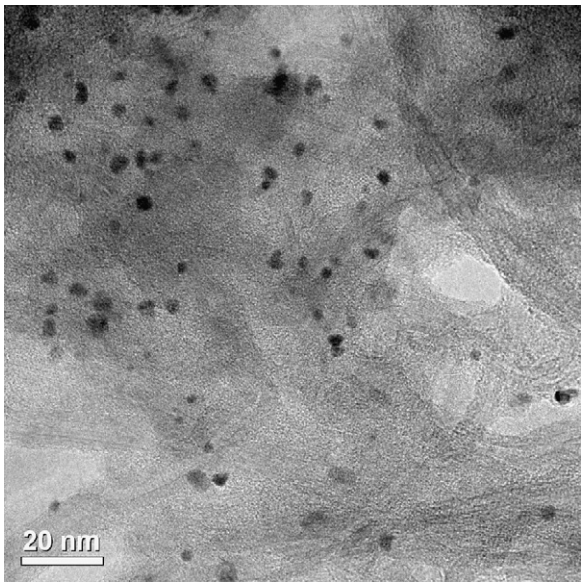


**Fig. 1.** TEM image of the PtAu/MWCNTs.

## 3. Results and discussion

### 3.1. Morphological characterization of the PtAu/MWCNTs nanocomposite

The micromorphology of the PtAu/MWCNTs catalyst was investigated by TEM, as depicted in Fig. 1. It can be seen from Fig. 1 that the nanoparticles were loaded on MWCNTs and distributed homogeneously. The size of the metal nanoparticles supported on MWCNTs is about 3.5 nm with narrow size distribution.

To investigate the components and chemical states of the prepared sample, X-ray photoelectron spectroscopy was adopted to characterize the sample. The XPS profiles of the PtAu/MWCNTs composite are shown in Fig. 2. As indicated in Fig. 2A, the prepared composite is mainly composed of C, Pt, and Au. In addition, the sample also contains a small amount of oxygen. This could be attributed to the functional groups such as –COOH and –OH on the modified MWCNTs. Fig. 2B and C is the XPS of Pt 4f and Au 4f in a selective location. From Fig. 2B, it can be clearly seen that the spectrum of Pt 4f consists of a doublet peak, corresponding to Pt $4f_{7/2}$ and Pt $4f_{5/2}$. The binding energy of Pt $4f_{7/2}$ and Pt $4f_{5/2}$ is 71.1 eV and 74.2 eV, respectively, which corresponds to metallic $Pt^0$ according to NIST XPS database. Meanwhile, Fig. 2C indicates that doublet peaks of Au $4f_{7/2}$ and Au $4f_{5/2}$ occur at 83.6 eV and 87.3 eV, respectively, which are smaller than their standard binding energy (83.70 eV and 87.38 eV). This may be attributed to the formation of PtAu-alloy.

Fig. 3 shows the XRD pattern of the PtAu/MWCNTs nanocomposite. A peak at $2\theta = 25.7°$ is assigned to graphitic carbon (0 0 2). The XRD pattern of the PtAu/MWCNTs catalyst exhibits three diffraction peaks at $2\theta$ values of 38.7°, 44.9° and 66.4°, respectively. It is interesting to note that the three diffraction peaks are not assigned to characteristic peak of Pt crystal and also not corresponding to characteristic peak of Au crystal. They located between the characteristic peaks of Pt crystal and Au crystal. It could also be attributed to the formation of alloy of Pt and Au on the MWCNTs.

### 3.2. Measurement of electroactive surface area

The electroactive surface area of Pt ($A_{Pt}$) was calculated by the charge of hydrogen adsorption/desorption, in which the charge density for hydrogen adsorption is known as 210 μC $cm^{-2}$ [27]. The charge for hydrogen adsorption ($Q_H$) on Pt surface sites can

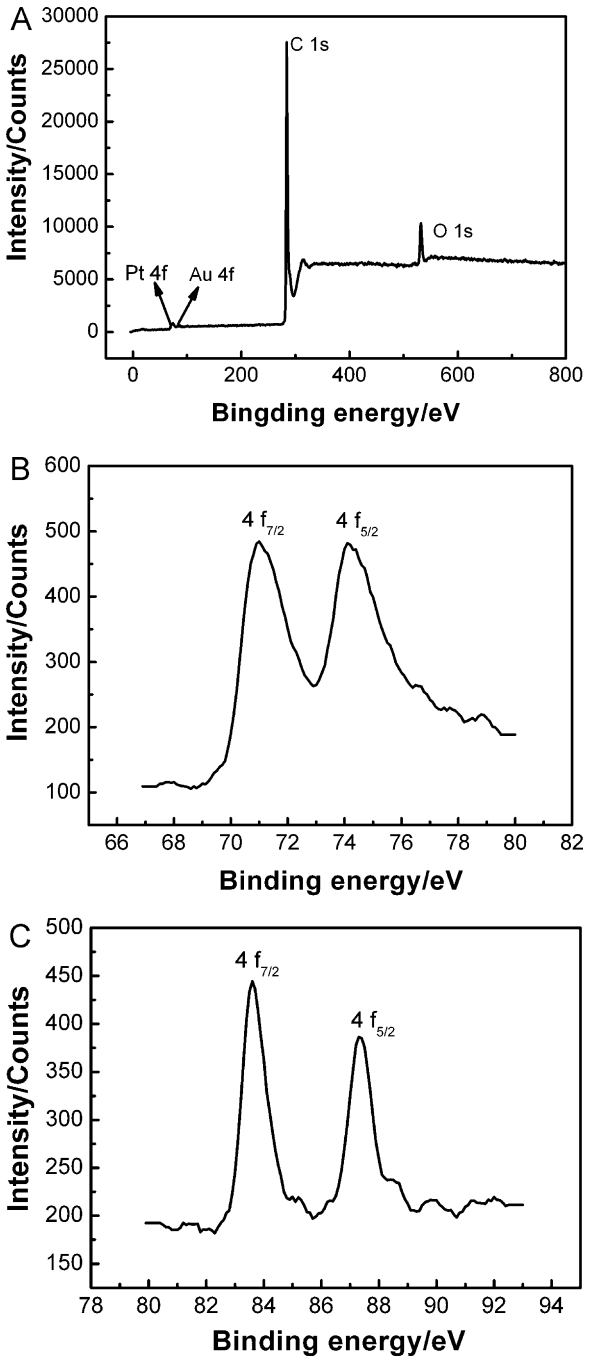


**Fig. 2.** XPS profiles of (A) PtAu/MWCNTs, (B) Pt 4f and (C) Au 4f.

be measured easily from the integration of current–potential curve appearing in the hydrogen adsorption potential region by CVs in 0.5 M $H_2SO_4$. Thus, we can easily obtain the $A_{Pt}$, which is equal to $Q_H$ divided by charge density (210 μC cm$^{-2}$). Therefore, in our experiments, the catalytic activity was shown directly through

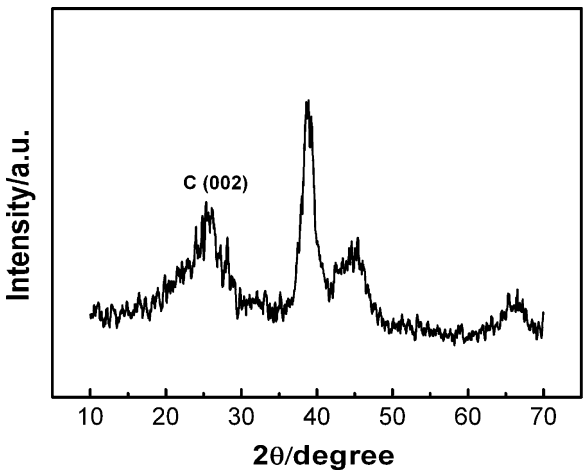


**Fig. 3.** XRD pattern of the PtAu/MWCNTs.

dividing the oxidation current by $A_{Pt}$. Any peak of hydrogen electro-oxidation in the CVs should arise from the presence of Pt component, as MWCNTs supported Au nanoparticles are inactive for the adsorption and electro-oxidation of hydrogen [28]. Therefore, the larger current density is, the higher catalytic activity is for per unit electroactive surface of Pt site. Besides, the influence of slight difference in size and amount of Pt nanoparticles on the glassy carbon electrode can be eliminated effectively by this way.

### 3.3. Evaluation of electro-oxidation of formic acid

In the experiments, the role of MWCNTs and Au/MWCNTs in electro-oxidation of HCOOH was first studied by CVs, as shown in Fig. 4. It can be seen that no additional peak appeared, when CVs were carried out with the MWCNTs and Au/MWCNTs electrodes in 0.50 M $H_2SO_4$ in the absence (black line) and presence (red line) of 0.50 M HCOOH. Therefore we conclude that MWCNTs and Au nanoparticles showed no catalysis directly towards the electro-oxidation of HCOOH.

Fig. 5 depicts the CVs for the PtAu/MWCNTs, commercial catalyst Pt/C and Pt/MWCNTs in 0.50 M $H_2SO_4$ solution with and without 0.50 M HCOOH in the potential range from −0.2 V to 1.0 V. The formic acid oxidation current was normalized to the electroactive surface area of Pt ($A_{Pt}$) loading on the MWCNTs and on the carbon. For the three electrodes, similar trends were observed, which showed two oxidation peaks (marked as $\alpha_1$ and $\alpha_2$) during the positive scanning and one oxidation peak (marked as $\beta$) during negative scanning. It indicates that the electro-oxidation of formic acid may follow an indirect dehydration conversion process which corresponds to a previous report [29], which reveals that electro-oxidation of HCOOH on Pt-based catalysts proceeds through a dual path mechanism that involves a direct dehydrogenation pathway and an indirect dehydration pathway. Peak $\alpha_1$ is attributed to the oxidation of adsorbed formate in indirect pathway on the active sites, and peaks $\alpha_2$ and $\beta$ may comprise the continuous oxidation of intermediate and adsorbed formate on the active sites free from intermediate CO*, respectively [30]. The mechanism of oxidation of

**Table 1**
Results of the electro-oxidation of formic acid at the PtAu/MWCNTs, Pt/MWCNTs and commercial Pt/C catalysts.

| Catalyst | $\alpha_1$ | | $\alpha_2$ | | $\beta$ | |
|---|---|---|---|---|---|---|
| | $E_{pa}$ (V) | $i_{pa}$ (mA cm$^{-2}$) | $E_{pa}$ (V) | $i_{pa}$ (mA cm$^{-2}$) | $E_{pa}$ (V) | $i_{pa}$ (mA cm$^{-2}$) |
| PtAu/MWCNTs | 0.42 | 3.12 | 0.75 | 2.52 | 0.60 | 7.34 |
| Pt/C | 0.33 | 0.14 | 0.72 | 0.61 | 0.47 | 1.50 |
| Pt/MWCNTs | 0.30 | 0.076 | 0.75 | 0.21 | 0.42 | 0.50 |

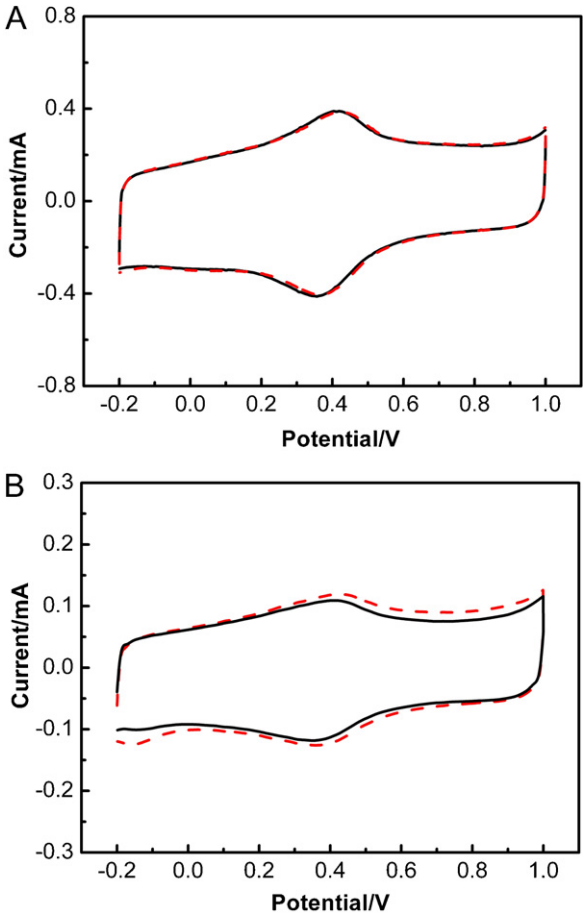


**Fig. 4.** CVs of MWCNTs (A) and Au/MWCNTs (B) electrodes in 0.50 M $H_2SO_4$ (solid line) and 0.50 M $H_2SO_4$ + 0.50 M HCOOH (dash line) solutions, scan rate: 50 mV/s.

formic acid on the PtAu/MWCNTs, Pt/C and Pt/MWCNTs electrodes is as follows:

$$HCOOH \rightarrow CO* + H_2O \quad (1)$$

$$CO* + Pt^0 \rightarrow Pt\text{–}CO* \quad (2)$$

$$Pt^0 + H_2O \rightarrow Pt\text{–}OH + H^+ + e \quad (3)$$

$$Pt\text{–}OH + Pt\text{–}CO* \rightarrow 2Pt^0 + CO_2 + H^+ + e^- \quad (4)$$

$$\text{Overall}: \quad HCOOH \rightarrow CO_2 + 2H^+ + 2e^- \quad (5)$$

As evidenced in Fig. 5, the PtAu/MWCNTs electrode exhibits much higher HCOOH oxidation current density than the commercial catalyst Pt/C and the Pt/MWCNTs electrodes. Especially, the first peak ($\alpha_1$) current density of oxidation of HCOOH at the PtAu/MWCNTs electrode is 3.12 mA cm$^{-2}$, while it is 0.14 mA cm$^{-2}$ at the commercial catalyst Pt/C and 0.076 mA cm$^{-2}$ at the Pt/MWCNTs electrodes. This indicates that the incorporation of Au nanoparticles greatly enhanced the utilization of Pt nanoparticles supported on MWCNTs. The results of the electro-oxidation of formic acid at the studied electrodes were summarized in Table 1. Meanwhile, it is noticed that the electro-oxidation of HCOOH mainly took place at low potential range from −0.05 V to 0.65 V on the PtAu/MWCNTs electrode (Fig. 5A), while at high potential range from 0.55 V to 1.0 V on the Pt/C and Pt/MWCNTs electrodes (Fig. 5B and C). The onset potential of oxidation of HCOOH at the PtAu/MWCNTs electrode is about −0.05 V, which shifts negatively about 150 mV compared to that at the commercial Pt/C and Pt/MWCNTs electrodes. The fact that both the electro-oxidation of HCOOH taking place at lower potential and onset potential shifting negatively discloses that the PtAu/MWCNTs electrode exhibits a higher catalytic activity for the electro-oxidation of HCOOH than that of the commercial Pt/C and Pt/MWCNTs. The incorporation of Au in Pt is of great benefit towards electro-oxidation of HCOOH.

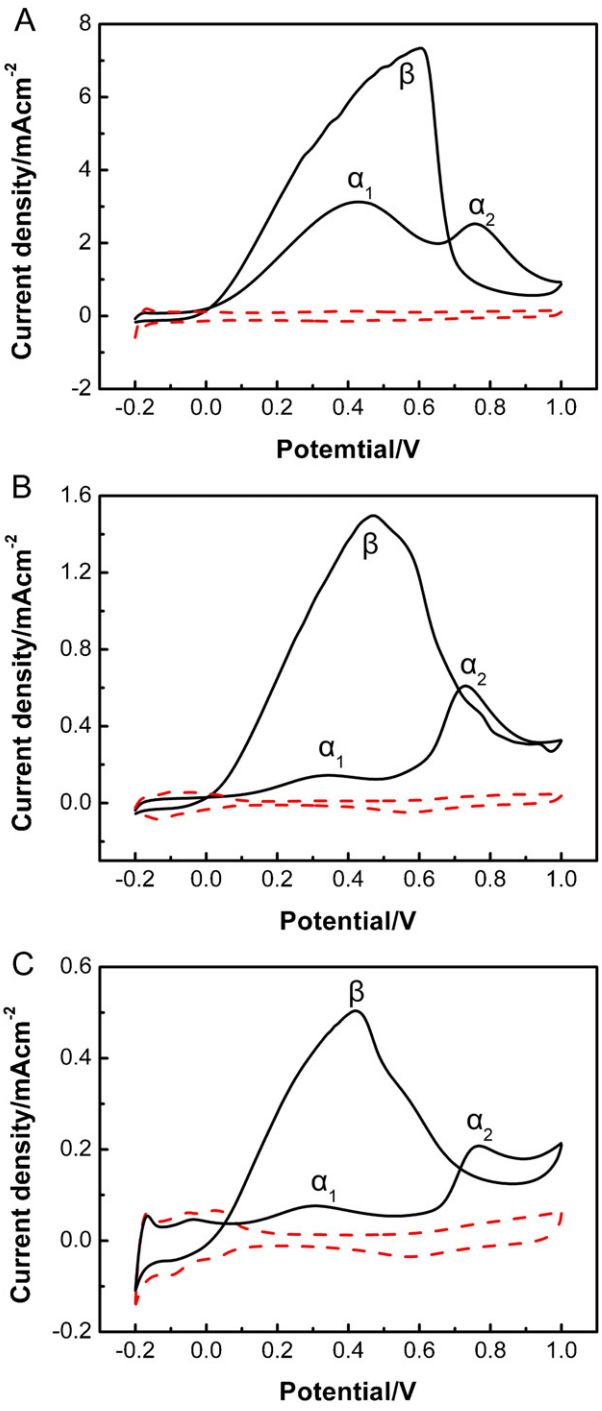


**Fig. 5.** CVs of the PtAu/MWCNTs (A), commercial catalyst Pt/C (B) and Pt/MWCNTs (C) electrodes in 0.50 M $H_2SO_4$ (dash line) and 0.50 M $H_2SO_4$ containing 0.50 M HCOOH (solid line), scan rate: 50 mV/s.

To investigate the stability of the PtAu/MWCNTs catalyst, commercial Pt/C catalyst and Pt/MWCNTs toward the electro-oxidation of HCOOH, chronoamperometry test was performed. Fig. 6 shows the chronoamperometry curves for the PtAu/MWCNTs, Pt/C and Pt/MWCNTs catalysts in 0.50 M $H_2SO_4$ solution in presence of 0.50 M HCOOH at the constant potential of 0.45 V for 2400 s. From Fig. 6, it can be seen that the current density decreased

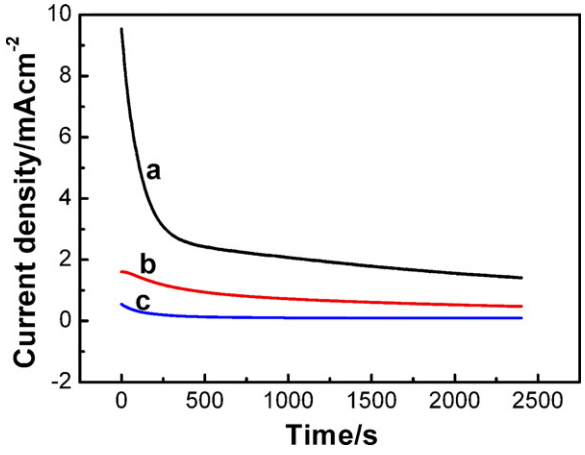


**Fig. 6.** Chronoamperometry curves of the PtAu/MWCNTs (a), commercial Pt/C (b) and Pt/MWCNTs (c) in 0.50 M $H_2SO_4$ containing 0.50 M HCOOH, applied potential: 0.45 V.

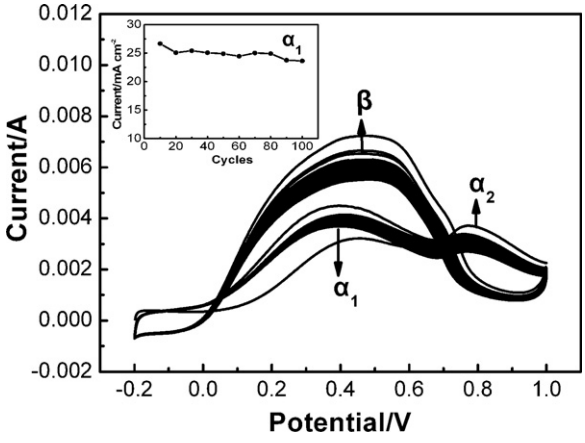


**Fig. 7.** CVs of the PtAu/MWCNTs in 0.50 M $H_2SO_4$ containing 0.50 M HCOOH for 100 cycles, scan rate: 100 mV/s; Inset: current density of peak $\alpha_1$ *vs* cycles.

rapidly for all the catalysts before 350 s, which can be due to some active sites occupied by intermediate species during the electro-oxidation of HCOOH. After that, the current density gradually decayed along the time, which may mainly result from the consumption of HCOOH during the reaction. It also could be due to poisoning and structure change of the PtAu nanoparticles as a result of perturbation of the potentials during the reaction, especially in the presence of the intermediate production during the oxidation of HCOOH [31]. The stable current density of PtAu/MWCNTs at 2000 s is 1.6 mA $cm^{-2}$, which is much higher than that of Pt/C (0.54 mA $cm^{-2}$) and Pt/MWCNTs (0.092 mA $cm^{-2}$), respectively. It reveals that introduction of Au to the nanocomposites endows the catalyst with much higher stable current density. In addition, CVs of the PtAu/MWCNTs in 0.50 M $H_2SO_4$ containing 0.50 M HCOOH for 100 circles were carried out to further confirm the stability of the PtAu/MWCNTs catalyst, and the result is indicated in Fig. 7. It is obvious that the current density of the peak $\alpha_1$ loses only 12.0% after 100 cycles.

### 3.4. CO stripping voltammetry

According to the previous CVs investigation, it was found that Au/MWCNTs showed no catalysis directly towards the oxidation of HCOOH. However, the activity of the PtAu/MWCNTs catalyst is remarkably higher than that of the Pt/MWCNTs. To study the role of Au in the PtAu/MWCNTs nanocomposite towards intermediate

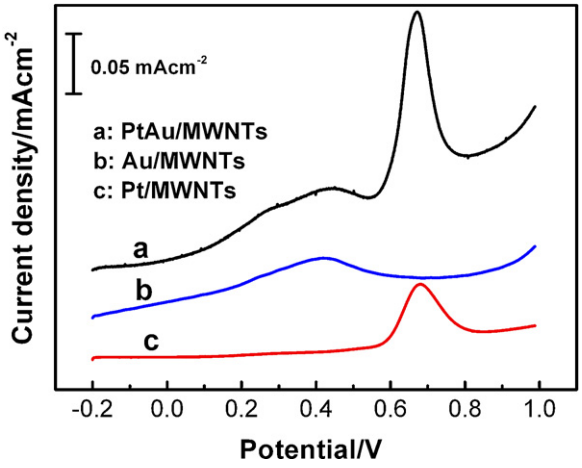


**Fig. 8.** CO stripping voltammogram curves of the PtAu/MWCNTs (a), Au/MWCNTs (b) and Pt/MWCNTs (c) electrodes in 0.50 M $H_2SO_4$ solution.

species (CO*), stripping voltammetry of CO at the PtAu/MWCNTs (Fig. 8a), Au/MWCNTs (Fig. 8b) and Pt/MWCNTs (Fig. 8c) electrodes was performed in 0.50 M $H_2SO_4$ solution. From Fig. 8, it can be observed that the hydrogen desorption peaks in the potential region from −0.2 V to 0.1 V are completely suppressed, which is due to the saturated coverage of CO species on the Pt active sites [32]. PtAu/MWCNTs and Pt/MWCNTs show catalytic activity to the oxidation of CO, but Au/MWCNTs does not. The peak current density of the PtAu/MWCNTs for electro-oxidation of CO is three times as high as that of the Pt/MWCNTs at 0.68 V. The increase of peak current density suggests that Au enhances the catalysis of PtAu/MWCNTs nanocomposite for electro-oxidation of CO. These results could be attributed to the synergism effects of Pt and Au [33–35]. Meanwhile, there is the possibility of a change in the electronic environment [35,36], which can affect the surface state of Pt. In addition, the presence of Au reduces the adsorption of poisoning species at the active sites by steric effects and the surface poisoning is thus suppressed [37]. The effect of Au on Pt catalytic activity needs further exploration in order to reach a definitive conclusion. More account for the dynamics of oxidation of CO process is desirable and further studies are undergoing.

## 4. Conclusion

In this study, PtAu/MWCNTs catalyst was successfully prepared by simultaneous reduction of $H_2PtCl_6{\cdot}6H_2O$ and $HAuCl_4{\cdot}3H_2O$ with sodium borohydride as a reducing reagent and sodium citrate as a stabilizing reagent. The prepared PtAu/MWCNTs showed higher electrocatalytic performance in electro-oxidation of HCOOH by occurring in the low potential range, higher peak current density and with good long-term performance, compared with the commercial catalyst Pt/C. Incorporation of gold into the nanocomposite catalyst enhanced its catalytic activity and the utilization of Pt. Therefore, PtAu/MWCNTs nanocomposite is a promising catalyst for the electro-oxidation of formic acid. It can also be the base of manufacturing other alloy catalysts for the direct fuel cells. The method reported in this article provides a solution to overcome the shortage of long-term stability of the catalysts for application in fuel calls.

## Acknowledgement

The authors would like to acknowledge Ministry of Science and Technology of China (2008AA06Z311) for financial support.

## References


[1] U.B. Demirci, J. Power Sources 169 (2007) 239–246.
[2] X. Wang, J.M. Hu, I.M. Hsing, J. Electroanal. Chem. 562 (2004) 73–80.
[3] M. Weber, J.T. Wang, S. Wasmus, R.F. Savinell, J. Electrochem. Soc. 143 (1996) L158–L160.
[4] C. Rice, S. Ha, R.I. Masel, A. Wieckowski, J. Power Sources 115 (2003) 229–235.
[5] P. Waszczuk, T.M. Barnard, C. Rice, R.I. Masel, A. Wieckowski, Electrochem. Commun. 4 (2002) 599–603.
[6] L.J. Zhang, Z.Y. Wang, D.G. Xia, J. Alloys Compd. 426 (2006) 268–271.
[7] E. Casado-Rivera, D.J. Volpe, L. Alden, C. Lind, C. Downie, T. Vazquez-Alvarez, A.C.D. Angelo, F.J. DiSalvo, H.D. Abruna, J. Am. Chem. Soc. 126 (2004) 4043–4049.
[8] E. Herrero, A. Fernández-Vega, J.M. Feliu, A. Aldez, J. Electroanal. Chem. 350 (1993) 73–88.
[9] Y.M. Zhu, Z. Khan, R.I. Masel, J. Power Sources 139 (2005) 15–20.
[10] N.M. Markovic, H.A. Gasteiger, P.N. Ross Jr., X. Jiang, I. Villegas, M.J. Weaver, Electrochim. Acta 40 (1995) 91–98.
[11] J. Clavilier, A. Fernández-Vega, J.M. Feliu, A. Aldaz, J. Electroanal. Chem. 258 (1989) 89–94.
[12] E. Rach, J. Heitbaum, Electrochim. Acta 32 (1987) 1173–1180.
[13] M. Valden, X. Lai, D.W. Goodman, Science 281 (1998) 1647–1650.
[14] J.H. Choi, K.J. Jeong, Y. Dong, J. Han, T.H. Lim, J.S. Lee, Y.E. Sung, J. Power Sources 163 (2006) 71–75.
[15] J.K. Lee, J. Lee, J. Han, T.H. Lim, Y.E. Sung, Y. Tak, Electrochim. Acta 53 (2008) 3474–3478.
[16] D. Zhao, B.Q. Xu, Angew. Chem. Int. Ed. 45 (2006) 4955–4959.
[17] T.W. Ebbesen, H.J. Lezec, H. Hiura, J.W. Bennett, H.F. Ghaemi, T. Thio, Nature 382 (1996) 54–56.
[18] Z.Z. Zhu, Z. Wang, H.L. Li, Appl. Surf. Sci. 254 (2008) 2934–2940.
[19] B. Yoon, C.M. Wai, J. Am. Chem. Soc. 127 (2005) 17174–17175.
[20] Y. Wen, J.S. Ye, W.D. Zhang, F.S. Sheu, G.Q. Xu, Microchim. Acta 162 (2008) 235–243.
[21] L.H. Li, W.D. Zhang, J.S. Ye, Electroanalysis 20 (2008) 2212–2216.
[22] L.M. Ang, T.S.A. Hor, G.Q. Xu, C.H. Tung, S.P. Zhao, J.L.S. Wang, Carbon 38 (2000) 363–372.
[23] E. Flahaut, A. Peigney, C. Laurent, A. Rouseet, J. Mater. Chem. 10 (2000) 249–252.
[24] M.S.P. Shaffer, X. Fan, A.H. Windle, Carbon 36 (1998) 1603–1612.
[25] N.R. Jana, L. Gearheart, C.J. Murphy, Langmuir 17 (2001) 6782–6786.
[26] M. Grzelczak, J. Pérez-Juste, P. Mulvaney, L.M. Liz-Marzán, Chem. Soc. Rev. 37 (2008) 1783–1791.
[27] N. Tian, Z.Y. Zhou, S.G. Sun, Y. Ding, Z.L. Wang, Science 316 (2007) 732–735.
[28] D.B. Laurence, Gold Bull. 37 (2004) 125–135.
[29] A. Capon, R. Parsons, J. Electroanal. Chem. 44 (1973) 239–254.
[30] H. Okamoto, W. Kon, Y. Mukouyama, J. Phys. Chem. B 109 (2005) 15659–15666.
[31] H.J. Wang, H. Yu, F. Peng, P. Lv, Electrochem. Commun. 8 (2006) 499–504.
[32] J.H. Jiang, A. Kucernak, J. Electranal. Chem. 543 (2003) 187–199.
[33] I.S. Park, K.S. Lee, D.S. Jung, H.Y. Park, Y.E. Sung, Electrochim. Acta 52 (2007) 5599–5605.
[34] J.H. Choi, K.W. Park, I.S. Park, K. Kim, J.S. Lee, Y.E. Sung, J. Electrochem. Soc. 153 (2006) A1812–A1817.
[35] D. Mott, J. Luo, P.N. Njoki, Y. Lin, L. Wang, C.J. Zhong, Catal. Today 122 (2005) 378–385.
[36] E. Bus, J.A.V. Bokhoven, J. Phys. Chem. C 111 (2007) 9761–9768.
[37] E. Leiva, T. Iwasita, E. Herrero, J.M. Feliu, Langmuir 13 (1997) 6287–6293.